UNCLASSIFIED

AD NUMBER
ADB270502
NEW LIMITATION CHANGE
TO Approved for public release, distribution unlimited
FROM Distribution authorized to U.S. Gov't. agencies only; Proprietary Information; JAN 1963. Other requests shall be referred to The National Aeronautics and Space Administration, Washington, DC 20546.
AUTHORITY
NASA ltr, 7 Nov 2005

THIS PAGE IS UNCLASSIFIED
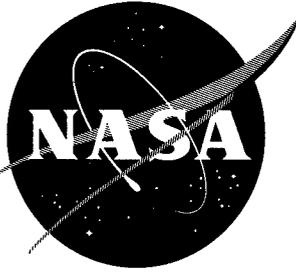
51783

TECHNICAL NOTE

D-1726

EXPERIMENTAL INVESTIGATION OF ROCKET-ENGINE ABLATIVE-

MATERIAL PERFORMANCE AFTER POSTRUN

COOLING AT ALTITUDE PRESSURES

By R. James Rollbuhler

Lewis Research Center
Cleveland, Ohio

PROPRIETARY INFORMATION

Jun
1963

DISTRIBUTION STATEMENT B
Distribution authorized to
U. S. Govt. Agencies Only
Other requests shall be referred to:
NASA, Washington, DC
20546

20010913 122

NATIONAL AERONAUTICS AND SPACE ADMINISTRATION

WASHINGTON   June 1963

NATIONAL AERONAUTICS AND SPACE ADMINISTRATION

TECHNICAL NOTE D-1726

EXPERIMENTAL INVESTIGATION OF ROCKET-ENGINE ABLATIVE-

MATERIAL PERFORMANCE AFTER POSTRUN

COOLING AT ALTITUDE PRESSURES

By R. James Rollbuhler

SUMMARY

An investigation was made to determine the effects of postrun cooling at simulated altitude pressures on ablative-rocket-material ablating characteristics.

Two identical ablative nozzles were test fired six times each (40-second tests) on the end of a 150-pound-thrust hydrogen-oxygen rocket engine at an absolute chamber pressure of 100 pounds per square inch. One nozzle cooled after each test in an ambient-pressure environment; the other nozzle cooled after each test while subjected to low-pressure vacuum conditions. The results are expressed in terms of nozzle weight loss, char-layer thickness, and internal-dimension changes.

Under the conditions of these tests, little noticeable effect occurred on the rates at which ablation materials erode either at sea-level pressures or at low pressures. In about 4 minutes of running, the throat area of each nozzle had essentially doubled, and the char was about 1/4-inch thick.

INTRODUCTION

Within the past few years, interest in using ablative materials for the combustion chamber and the nozzle walls of rocket engines has intensified. A few of the advantages of using ablative materials to maintain the physical integrity of a rocket engine are increased versatility in varying the propellant flows by elimination of regenerative cooling requirements, simplicity of the propellant-flow systems, and rapidity of engine development.

The use of ablative materials in production engines has thus far been confined to those portions of rocket engines that are difficult or impossible to cool regeneratively, for example, engine throats or solid-propellant rocket nozzles. The materials used have been carbon, graphite, or refractory metals. Recently, however, new ablative materials, which consist of mixtures of plastic resin binder and silica or graphite fiber reinforcement, have been developed for the fabrication of entire chambers (refs. 1 to 3).

One area of concern, which has only been lightly explored, is the effect of low pressures, such as would be found in space, on ablative chambers, particularly when the ablation material is still hot, following a run. The resins in these proposed ablative materials start to decompose when their temperatures rise above 300° to 400° F at a pressure of 1 atmosphere. After a run, the wall temperature of an ablative rocket engine can theoretically be greater than 1500° F. These organic resins could possibly volatilize at an extreme rate until they cooled below their decomposition temperatures. Such volatilization would theoretically be even greater when in the vacuum conditions of space. Madorsky and Straus (ref. 4) have reported that a typical phenolic resin, when heated in a vacuum furnace for 5 minutes, was volatilized 29 percent at 930° F and was volatilized 47 percent at 1470° F. More material did not volatilize only because a carbonaceous char layer formed over the surface.

Previous efforts to investigate this problem by use of ablative materials have consisted of heating small pieces electrically in a vacuum apparatus to temperatures up to 300° F (ref. 5) or of heating samples with a torch and then putting them in a vacuum atmosphere (ref. 6). These test methods reported no important effects due to cooling in a vacuum as compared with cooling at atmospheric pressure (less than 1 percent difference in weight loss). Such methods, however, do not reproduce the actual conditions that may be encountered in a full-size rocket engine operating in deep space. For example, the high shear forces encountered in a rocket nozzle may have a serious effect on the erosion rate of ablative materials. Conditions of combustion-gas composition and temperature environment cannot be duplicated without actual use of a rocket engine.

This investigation was made to determine experimentally if rocket engines, which contain ablative materials, would be affected detrimentally by cooling after each run in a low-pressure vacuum atmosphere as compared with cooling at a pressure of 1 atmosphere. Two identical ablative nozzles were tested six times each on the end of a 150-pound-thrust (100 lb/sq in. abs chamber pressure) hydrogen-oxygen rocket engine. One nozzle cooled after each test while it was at ambient pressure; the other nozzle cooled after each test while it was subjected to low-pressure conditions. The results of these tests are expressed in terms of nozzle weight losses, char-layer thicknesses, and internal-dimension changes.

APPARATUS

Test Facility

This investigation was conducted in a test facility capable of supplying hydrogen and oxygen at liquid-nitrogen temperatures. For ignition purposes, a gaseous fluorine supply was available. The flow systems and the hardware were so sized that chamber pressure equaled 100 pounds per square inch absolute; total propellant flow was about 1/2 pound per second; and the fuel was 15 percent by weight of the total propellant. Thrust was a nominal 150 pounds. All test runs were made with the combustion gases exhausting to the atmosphere.

The propellant-flow systems and the vacuum environment equipment are shown schematically in figure 1. The gaseous hydrogen was supplied from high-pressure gas cylinders. The flow rate was controlled by a pressure regulator. Prior to

engine injection, the hydrogen was cooled by passing it through a liquid-nitrogen heat exchanger. This method closely simulated the conditions of liquid-hydrogen use in space engines.

The oxidant system consisted of a propellant supply source that was connected to the engine through two flowmeters and a fire valve. The entire system was submerged in liquid nitrogen.

The fluorine ignition system was a fluorine gas cylinder connected by suitable valving to the oxidant side of the engine injector.

The method of supplying space-environment pressures to the engine interior during cooling is shown at the bottom of figure 1. The rocket engine fired into a zirconium-oxide-coated, 8-inch-diameter pipe that had an 8-inch gate valve on the exhaust end. Tied into the 8-inch pipe was a line that connected it to a 200-cubic-foot vacuum surge tank. A valve in this line isolated the surge tank from the 8-inch pipe. Vacuum was obtained in the entire system by a rotary-piston vacuum pump with a capacity of 40 cubic feet per minute.

Engines

The rocket engines used in this investigation consisted of three pieces - an injector, a cooled combustion chamber, and the ablation nozzle that was tested. The three pieces are shown in figure 2. They were held together during a run by pneumatic clamps.

The injector used was a 12-element concentric-tube type consisting of 12 axial oxygen jets, each surrounded by a hydrogen annulus, in concentric rings of 8 and 4 elements each. This injector was checked out initially with engines having steel heat-sink nozzles. The results of such tests were compared with those obtained with triplet, showerhead, swirl-cup, doublet, and nine-element concentric-tube (injector shown in fig. 2) injectors. The 12-element injector caused less erosion or gouging of the checkout nozzles than did any of the other injectors at a high-performance level.

The combustion chamber was a 4-inch-long cylinder with a water-coolant jacket. A chamber pressure tap was located on the chamber near the injector. This chamber minimized any effect of combustion-gas recirculation, injector spray impingement, and starting variation on the ablation material.

The two ablation nozzles, identified as 9 and 10, were machined from a single block of phenolic-high-purity-silica-fiber material (fig. 3). The block was formed of layers of silica-fiber cloth that had been coated with phenolic resin and then bonded under high pressure. The centerline of each nozzle was perpendicular to the layers of bonded cloth. Each nozzle had a converging section with an included angle of 24° and a 1- by 1.2-inch-diameter tubular throat. The nozzles had no diverging section.

Instrumentation

During the runs, primary data were taken on the hydrogen and the oxygen flow rates, the combustion-chamber pressure, and the ablation-material wall temperatures. Secondary data were taken of the fuel- and oxidant-injection pressures and temperatures, fluorine-ignitor flow rate, and time of engine ignition and shutdown. After engine shutdown, continuous data were taken on the ablation wall temperatures and the nozzle vacuum pressure.

Pressures, both static and differential, were measured with strain-gage pressure transducers that were accurate to ±2 percent of full scale. Flow rates were determined from the pressure differentials across orifice plates in both the fuel and the oxidant flow lines. In the oxidant system, a turbine-type flowmeter was used as a backup data source. The accuracy of the flow data from any of the flowmeters was approximately ±2 percent.

Temperatures of the cryogenic propellants were measured with copper-constantan thermocouples, which had an estimated accuracy of ±5°. The ablative wall-temperature data were obtained from 12 Chromel-Alumel thermocouples buried in the material. The thermocouples were at three axial planes; at each plane, the four thermocouples were 90° apart. The locations of these planes are shown in figure 4, and the distance from the tip of each thermocouple to the inner surface is given in table I. These thermocouples supplied data that were about ±2 percent accurate.

All the pressure-transducer and thermocouple data were recorded on a multi-channel, variable-speed oscillograph recorder. The three primary-run variables, oxidant flow rate, fuel flow rate, and chamber pressure, were also recorded on self-balancing potentiometer strip charts. The internal-surface dimensions and the char-layer thickness were measured from X-rays taken of each nozzle after each run. The nozzles were weighed between runs to an accuracy of ±1/2 gram.

TEST PROCEDURE

Prior to actual running, the instrumentation equipment was calibrated and the assembled engine was pressure checked. To obtain the desired flow rates of propellants during the run, the fuel and oxidant systems were pressurized to known values.

The run itself was programed automatically by a sequence timer. The fluorine ignition, which was used less than 1 second, gave smooth starts and apparently had no effect on the ablative nozzle material.

After each run nozzle 9 was allowed to cool at ambient pressures before being removed from the test rig. When nozzle 10 was tested, the 8-inch gate valve at the end of the firing pipe was closed immediately after the run. The valve took 17 seconds to close, during which time the propellant systems were purged through the engine. As soon as the valve was closed, the automatic valve in the line between the firing pipe and the vacuum tank was opened. The vacuum tank had been evacuated to a pressure of approximately 1/2 millimeter of mercury prior to the run. Thus, the engine interior was exposed to low-pressure conditions 17 seconds

after the run ended. The interior was kept at as low a pressure as possible for at least 1 hour after the run. During this hour, the nozzle wall temperatures and the nozzle interior pressure were monitored continuously. After cooling down, the engine was disassembled, and the nozzle was weighed and X-rayed.

RESULTS AND DISCUSSION

The primary conditions of the runs with each nozzle are presented in table II. This table includes the run-duration time, the maximum and the minimum chamber pressures, the percentage of fuel in the total propellant flow, and the maximum characteristic velocity. The characteristic velocity was calculated when the running conditions of each run had stabilized, usually 5 to 10 seconds after ignition. This velocity was calculated on the basis of the prerun nozzle throat cross-sectional area, the maximum chamber pressure, and the total propellant-flow rate at that chamber pressure. After the first 10 seconds of run time, the throat area had changed from prerun values and the characteristic-velocity data could no longer be determined accurately. The minimum chamber pressure was that recorded just prior to run termination.

During each run, the propellant-flow rates were kept approximately constant; however, as the nozzle-throat erosion increased for each run, it became impossible, because of flow-system limitations, to increase both propellant-flow rates enough to maintain the chamber pressure of the initial run. Consequently, by the last run of each nozzle, the chamber pressure was about 65 rather than 100 pounds per square inch absolute, and the percentage of fuel in the total propellant flow had decreased from about $15\frac{1}{2}$ to 12.

Despite these difficulties, the characteristic velocity was greater than 94 percent of theoretical equilibrium performance (table II). Results of an unpublished Lewis investigation show that the ablation rate is a strong function of the combustion temperature, which, in turn, is related to the characteristic-velocity efficiency. For example, at a chamber pressure of 100 pounds per square inch absolute and about 15-percent fuel in the total propellant flow of a hydrogen-oxygen rocket, the theoretical combustion temperature is approximately 5100° F at 100-percent combustion efficiency and 4700° F at 90-percent combustion efficiency. Therefore, on the basis of the efficiencies obtained during each run, the nozzles were tested under realistic ablation conditions.

The runs were limited to 40 seconds in duration because of overheating of the coated 8-inch pipe into which the test engine fired.

Nozzle internal dimensions were measured from X-rays taken of each nozzle after each run. Figures 4(a) to (d) are typical examples. Actually, two X-rays were taken every time at 90° angles to each other so that a parallel view of all the thermocouples would be obtained. The internal surface radii were measured in both X-rays at the three thermocouple planes, and at each plane the four measured radii were averaged. This average radius for each plane is presented in table II for each nozzle after each run. The radii were averaged in order to eliminate the effect of occasional grooving of nozzle walls, which is attributed to askew oxidant injection jets. Such grooving was minimized by reaming out the jet

orifices and by rotating the nozzle (with respect to the injector) between runs. The rate at which these radii increased as a function of run duration is also presented in table II.

From the same X-ray, the char-layer thickness can also be measured. It shows as a difference of intensity in the X-rays. The char thickness is presented for each nozzle after each run in table II. Again these values are averaged at each of the three thermocouple planes in the nozzle.

Photographs of nozzles 8 and 10, after their sixth and final runs, are shown in figures 5(a) and (b), respectively. Clearly visible on the internal surface of each nozzle is the resolidified silica, which melted and started flowing downstream during the run. This behavior of the silica occurred when the greatest erosion was taking place. Other ablative nozzles, which were operated at lower combustion temperatures, had a gray-ash appearance after tests and had very little physical erosion. Numerous small separations between the plys of the nozzle-wall material at the inner surface are visible in the X-rays (figs. 4(c) and (d)) but not in the photographs as the flowing silica has covered them. Figure 5(c) is a photograph of half of each nozzle after final tests. The interface, or boundary, between the char and the virgin material shows clearly, and measurements agree with the previously mentioned measurements made from the X-rays. The char layer appears the thickest at those surfaces where the erosion rate is the least.

During and after the running of each of the nozzles, temperature data were obtained from the thermocouples buried at various depths in the nozzle walls. These data are reported for each run in table I at selected time increments. Data given in table I(a) are from tests made with nozzle 9, and data given in table I(b) were obtained when nozzle 10 was used. Also given in table I are the prerun and postrun radial thermocouple depths (from the inner surface). These depths were measured from the postrun X-rays of each nozzle (e.g., fig. 4). Some of the thermocouples shorted, broke, or the signal went over range on the recorder during one or all of the runs (e.g., thermocouples 1 and 2). These mishaps are indicated in table I by a blank in the data. Some of the temperature data show sudden changes, increases or decreases, which suggest the possibility of ablation wall cracks that expose the thermocouple directly to the combustion-chamber environment. These cracks appear in the X-rays of each nozzle, for example, thermocouple 3 in figure 4(d).

A better perspective of the nozzle-wall temperature patterns is shown by a plot of the temperature data from a single arbitrarily selected measuring plane B in figure 6 as a function of the postrun thermocouple depth. The figure includes data from all the tests with each nozzle. The data presented in figure 6 are at 40, 60, 240, and 480 seconds after the start of each run. Each run ended approximately 40 seconds after the start. These figures indicate that both nozzles had similar wall-temperature gradients at the time and the measuring plane that were considered. Examination and comparison of the temperature data for other planes and times give similar results. Thus, postrun pressure appears to have little effect on the heating and the cooling characteristics of ablative material. It can be surmised from figures 6(a) and (b) that the temperature of approximately 600° F at the interface between the char and the virgin material is within the decomposition temperature range for phenolic resin. Although low-pressure vacuum

could not be applied to the internal ablation surface of nozzle 10 until more than 17 seconds after the end of each run, figure 6(b) indicates that the extrapolated surface temperature was greater than 2000° F and that the char-virgin-material interface temperature was approximately the same as at the conclusion of the run. As cooling proceeded, the ablation walls established a more uniform temperature gradient.

The pressure on the downstream end of nozzle 10, which was cooled after each run while it was exposed internally to a low-pressure vacuum environment, is tabulated in table I(b) for selected times during and after each run. Data during the runs indicate that as the engine fired down the coated pipe, an aspirated or low-pressure effect was produced on the end of the nozzle. As soon as the valve on the end of this pipe had closed (17 sec after each run), the interior of the engine was exposed to a pressure of less than 10 millimeters of mercury absolute. After each run, however, the valve on the end of the coated pipe leaked more and more. Consequently, as can be seen from the pressure data in table I(b), the initial vacuum pressure gradually increased because of valve leakage rates that the system vacuum pump could not handle. Only after sealing material was packed around the valve gate seals did that pressure decrease. Fortunately, the best obtainable vacuum was achieved when the ablation material was the hottest.

The effects of postrun pressures on subsequent ablation performance of the ablation nozzles is shown in figure 7. In this figure the average radius at the nozzle-throat entrance (plane B) of both nozzles 9 (cooled at ambient pressure) and 10 (cooled at low pressure) are plotted as a function of accumulated run time. One set of radii is from the nozzle centerline to the char-material - hot-gas surface, and the other is the radius from the centerline to the char-virgin-material interface. For both nozzles the radius at this plane, as well as at the other two planes, increases at about the same rate - 0.0006 to 0.0026 inch per second of running time. After the initial run for each nozzle, the char-virgin-material interface progressed at about the same rate as the surface erosion. The char thickness remained about 1/4 inch. Thus, no significant difference was found in the rates of ablation under cooling down exposures to vacuum or to atmospheric pressures.

The postrun weight of each nozzle is plotted as a function of accumulated run time for both nozzles in figure 8. Both nozzles lost weight at approximately the same rate. After almost 4 minutes of run time, each nozzle had lost 6 to 7 percent of its initial weight. Therefore, on the basis of weight lost, no significant difference occurred, and the results obtained from X-ray measurements are supported.

CONCLUSIONS

An investigation was conducted to establish quickly whether conditions of cooling down in a vacuum had a serious effect on the subsequent behavior of an ablative material used as an integral part of a rocket engine that fired intermittently. Under the limitations of the experimental program (e.g., 17-sec postrun delay in obtaining vacuum conditions), cooling at low pressure as compared with cooling at atmospheric pressure had little noticeable effect on the ablative material.

From this limited investigation, there appears to be no reason to believe a drastic failure of an ablative chamber will occur in space because of a vacuum environment.

REFERENCES

1. Lonon, D. N., and Olcott, G.: Research and Development of Components for Pressure-Fed Liquid Oxygen - Liquid Hydrogen Upper-Stage Propulsion Systems. Task I - Ablative-Thrust-Chamber Feasibility Firings. Rep. 1933, Aerojet-General Corp., Feb. 1961.

2. Staff of Liquid Rocket Branch, Engineering Division: Thrust Chamber Cooling by the Ablation Process. United Tech. Corp., June 26, 1961.

3. Lyons, C. S., and Lawson, D. D.: Ablative Characteristics of Reinforced Plastics in Nozzles and Thrust Chambers for Varying Environments. North Am. Aviation, 1962.

4. Madorsky, Samuel L., and Straus, S.: Thermal Degradation of Polymers at Temperatures up to 1200° C. TR 59-64, pt. II, WADC, Mar. 1960.

5. Wahl, Norman E.: Effect of Ultraviolet and Vacuum on Properties of Platics. TR 60-101, WADD, Sept. 1960.

6. Gray, P. D., et al.: Rockets in Space Environment. Phase II: Individual Component Investigation. Rep. 2263, Aerojet-General Corp., Apr. 11, 1962.

Lewis Research Center
    National Aeronautics and Space Administration
        Cleveland, Ohio, February 26, 1963

TABLE I. - INTERNAL-WALL TEMPERATURES AND

(a) Ablation

Run	Time after start of run, sec	Plane C (2 in. from nozzle exit)				Plane B (1 in. from nozzle exit)					
		Thermocouple									
		3		4		5		6		7	
		Temperature, °F	Distance from inner surface, mm	Temperature, °F	Distance from inner surface, mm	Temperature, °F	Distance from inner surface, mm	Temperature, °F	Distance from inner surface, mm	Temperature, °F	Distance from inner surface, mm
1875	0	64	8.0	55	13.0	49	8.0	56	14.0	50	16.5
	5	64	---	60	----	49	---	50	----	47	----
	10	67	---	60	----	49	---	58	----	53	----
	20	85	---	58	----	55	---	56	----	47	----
	30	131	---	67	----	230	---	61	----	50	----
	60	210	---	85	----	455	---	88	----	60	----
	120	260	---	120	----	610	---	135	----	55	----
	180	305	---	222	----	625	---	240	----	115	----
	240	296	---	252	----	550	---	269	----	167	----
	600	---	---	219	----	360	---	258	----	221	----
	1200	---	---	176	----	250	---	215	----	200	----
	2100	---	---	153	----	160	---	172	----	163	----
	3600	---	7.0	121	13.0	90	8.0	130	13.0	124	16.5
1878	0	70	7.0	65	13.0	63	8.0	67	13.0	56	16.5
	10	76	---	60	----	118	---	86	----	52	----
	20	135	---	70	----	210	---	72	----	54	----
	30	242	---	83	----	360	---	102	----	54	----
	40	361	---	121	----	---	---	155	----	60	----
	50	215	---	187	----	---	---	205	----	60	----
	60	242	---	238	----	---	---	257	----	98	----
	90	508	---	325	----	---	---	322	----	105	----
	180	495	---	360	----	---	---	367	----	215	----
	240	401	---	352	----	390	---	375	----	272	----
	480	253	---	235	----	242	---	268	----	217	----
	900	185	---	176	----	170	---	190	----	202	----
	1800	131	---	121	----	108	---	129	----	115	----
	3600	94	7.0	86	12.0	90	[a]4.5	89	12.0	78	13.5
1880	0	73	7.0	46	12.0	75	[a]4.5	70	12.0	58	13.5
	5	87	---	24	----	117	---	70	----	57	----
	10	210	---	43	----	233	---	72	----	57	----
	20	315	---	47	----	540	---	113	----	58	----
	30	455	---	53	----	---	---	147	----	70	----
	40	584	---	69	----	---	---	198	----	92	----
	50	720	---	72	----	---	---	325	----	177	----
	60	713	---	81	----	---	---	363	----	225	----
	90	663	---	90	----	---	---	410	----	290	----
	120	614	---	122	----	---	---	437	----	326	----
	240	437	---	64	----	405	---	421	----	346	----
	480	315	---	---	----	285	---	349	----	300	----
	900	219	---	---	----	215	---	261	----	233	----
	1440	195	[a]6.5	---	11.0	170	[a]5.0	202	11.5	187	12.0

[a]In char layer.

THERMOCOUPLE RADIAL DISTANCE FROM INNER SURFACE

nozzle 9.

Plane A (1/2 in. from nozzle exit)									
Thermocouple									
8		9		10		11		12	
Temperature, °F	Distance from inner surface, mm	Temperature, °F	Distance from inner surface, mm	Temperature, °F	Distance from inner surface, mm	Temperature, °F	Distance from inner surface, mm	Temperature, °F	Distance from inner surface, mm
61	22.5	60	22.0	62	6.0	57	13.0	60	----
60	----	61	----	65	---	53	----	56	----
63	----	67	----	95	---	60	----	60	----
61	----	62	----	143	---	57	----	65	----
60	----	65	----	578	---	66	----	66	----
62	----	65	----	695	---	85	----	60	----
70	----	70	----	630	---	145	----	75	----
85	----	175	----	545	---	260	----	200	----
122	----	197	----	477	---	284	----	264	----
210	----	256	----	320	---	265	----	288	----
200	----	210	----	229	---	204	----	230	----
167	----	162	----	180	---	161	----	179	----
125	22.5	122	21.5	130	5.5	122	13.0	134	17.0
66	22.5	67	21.5	---	5.5	70	13.0	73	17.0
61	----	67	----	---	---	70	----	66	----
66	----	67	----	---	---	72	----	70	----
66	----	67	----	---	---	84	----	70	----
66	----	68	----	---	---	123	----	75	----
72	----	70	----	---	---	185	----	72	----
71	----	80	----	---	---	217	----	112	----
92	----	135	----	---	---	300	----	163	----
123	----	175	----	---	---	103	----	220	----
197	----	275	----	---	---	347	----	288	----
185	----	208	----	---	---	253	----	224	----
162	----	162	----	---	---	180	----	171	----
117	----	116	----	---	---	---	----	125	----
84	18.5	85	19.0	---	[a]4.5	---	10.0	87	14.5
68	18.5	69	19.0	---	[a]4.5	73	10.0	73	14.5
68	----	69	----	---	---	73	----	75	----
70	----	69	----	---	---	82	----	73	----
72	----	73	----	---	---	114	----	75	----
70	----	72	----	---	---	181	----	83	----
70	----	78	----	---	---	223	----	106	----
90	----	117	----	---	---	410	----	200	----
105	----	147	----	---	---	463	----	264	----
142	----	207	----	---	---	550	----	305	----
182	----	253	----	---	---	556	----	392	----
271	----	327	----	---	---	469	----	403	----
262	----	285	----	---	---	348	----	312	----
217	----	222	----	---	---	251	----	232	----
162	17.5	182	19.0	---	[a]4.5	202	8.5	195	12.5

TABLE I. - Continued. INTERNAL-WALL TEMPERATURES

(a) Concluded.

Run	Time after start of run, sec	Plane C (2 in. from nozzle exit)				Plane B (1 in. from nozzle exit)					
		Thermocouple									
		3		4		5		6		7	
		Temperature, °F	Distance from inner surface, mm	Temperature, °F	Distance from inner surface, mm	Temperature, °F	Distance from inner surface, mm	Temperature, °F	Distance from inner surface, mm	Temperature, °F	Distance from inner surface, mm
1882	0	70	[a]6.5	66	11.0	55	[a]5.0	69	11.5	57	12.0
	5	95	---	69	----	188	---	70	----	59	----
	10	229	---	66	----	360	---	118	----	57	----
	20	340	---	128	----	---	---	150	----	59	----
	30	460	---	204	----	---	---	209	----	73	----
	40	577	---	245	----	---	---	228	----	114	----
	50	642	---	340	----	---	---	270	----	185	----
	60	660	---	430	----	---	---	362	----	240	----
	90	605	---	475	----	---	---	390	----	305	----
	120	402	---	389	----	418	---	408	----	325	----
	240	331	---	332	----	340	---	352	----	292	----
	480	255	---	240	----	255	---	283	----	236	----
	900	108	---	163	----	170	---	205	----	175	----
	1800	133	[a]6.0	96	11.5	125	[a]4.5	133	9.0	115	12.0
1884	0	50	[a]6.0	68	11.5	---	[a]4.5	72	9.0	57	12.0
	5	60	---	69	----	780	---	71	----	56	----
	10	120	---	79	----	1380	---	101	----	60	----
	20	205	---	175	----	2140	---	226	----	67	----
	30	305	---	284	----	2280	---	254	----	76	----
	40	350	---	423	----	1860	---	287	----	99	----
	50	425	---	565	----	1305	---	330	----	90	----
	60	465	---	611	----	1120	---	366	----	156	----
	90	490	---	610	----	820	---	480	----	185	----
	120	445	---	553	----	670	---	499	----	260	----
	240	360	---	433	----	430	---	440	----	295	----
	480	245	---	279	----	260	---	339	----	266	----
	900	160	---	207	----	130	---	237	----	201	----
	1500	100	[a]6.5	150	6.5	70	[a]2.5	169	9.0	147	12.0
1886	0	40	[a]6.5	62	6.5	---	[a]2.5	72	9.0	67	12.0
	5	50	---	172	----	---	---	72	----	63	----
	10	160	---	175	----	---	---	108	----	64	----
	20	330	---	327	----	---	---	207	----	65	----
	30	535	---	587	----	---	---	259	----	70	----
	40	665	---	807	----	---	---	319	----	128	----
	50	795	---	860	----	---	---	370	----	140	----
	60	810	---	812	----	---	---	415	----	227	----
	90	750	---	700	----	---	---	540	----	280	----
	120	665	---	606	----	---	---	542	----	356	----
	240	450	---	417	----	---	---	458	---	356	----
	480	295	---	288	----	---	---	340	---	289	----
	900	170	---	182	----	---	---	227	---	210	----
	1800	75	[a]6.0	111	[a]4.0	---	[a]2.0	138	[a]7.0	134	12.0

[a]In char layer.

Ablation nozzle 9.

			Plane A (1/2 in. from nozzle exit)						
				Thermocouple					
8		9		10		11		12	
Temperature, °F	Distance from inner surface, mm	Temperature, °F	Distance from inner surface, mm	Temperature, °F	Distance from inner surface, mm	Temperature, °F	Distance from inner surface, mm	Temperature, °F	Distance from inner surface, mm
70	17.5	70	19.0	72	^{a}4.5	74	8.5	74	12.5
74	----	70	----	310	---	84	----	80	----
74	----	70	----	711	---	97	----	78	----
66	----	70	----	1346	---	160	----	83	----
70	----	70	----	1623	---	247	----	109	----
80	----	77	----	1810	---	337	----	172	----
95	----	95	----	1600	---	405	----	225	----
135	----	121	----	1228	---	476	----	324	----
185	----	185	----	970	---	490	----	384	----
280	----	307	----	547	---	400	----	378	----
490	----	512	----	432	---	555	----	547	----
220	----	224	----	310	---	265	----	244	----
160	----	161	----	198	---	189	----	170	----
123	15.0	120	18.0	132	^{a}2.0	127	9.0	125	10.0
71	15.0	72	18.0	63	^{a}2.0	77	9.0	73	10.0
71	----	72	----	670	---	67	----	75	----
71	----	75	----	1205	---	78	----	77	----
72	----	80	----	1690	---	92	----	110	----
79	----	75	----	1950	---	101	----	190	----
95	----	82	----	2010	---	113	----	291	----
145	----	105	----	1675	---	130	----	430	----
182	----	136	----	1475	---	145	----	484	----
270	----	220	----	1090	---	205	----	530	----
306	----	271	----	905	---	225	----	997	----
328	----	315	----	580	---	363	----	407	----
264	----	255	----	330	---	179	----	387	----
187	----	182	----	205	---	---	----	---	----
145	11.5	142	----	120	^{a}1.5	155	8.5	141	6.5
72	11.5	65	----	47	^{a}1.5	---	8.5	72	6.5
78	----	63	----	46	---	---	----	68	----
156	----	65	----	46	---	---	----	74	----
257	----	67	----	46	---	---	----	87	----
544	----	83	----	1890	---	---	----	142	----
843	----	124	----	2170	---	---	----	191	----
920	----	185	----	1820	---	---	----	245	----
851	----	240	----	1510	---	---	----	266	----
740	----	335	----	1125	---	---	----	405	----
630	----	354	----	890	---	---	----	423	----
422	----	337	----	530	---	---	----	378	----
287	----	252	----	300	---	---	----	288	----
193	----	181	----	185	---	---	----	203	----
122	9.0	113	10.5	70	^{a}1.0	---	8.5	133	^{a}4.0

TABLE I. - Continued. INTERNAL-WALL TEMPERATURES

(b) Ablation

Run	Time after start of run, sec	Plane C (2 in. from nozzle exit)				Plane B (1 in. from nozzle exit)					
		Thermocouple									
		3		4		5		6		7	
		Temperature, °F	Distance from inner surface, mm	Temperature, °F	Distance from inner surface, mm	Temperature, °F	Distance from inner surface, mm	Temperature, °F	Distance from inner surface, mm	Temperature, °F	Distance from inner surface, mm
1876	0	66	9.0	---	13.0	68	8.5	58	11.5	50	18.5
	5	67	---	62	----	68	---	61	----	50	----
	10	69	---	64	----	72	---	61	----	53	----
	20	86	---	64	----	90	---	61	----	53	----
	30	133	---	69	----	139	---	72	----	47	----
	50	210	---	88	----	230	---	105	----	50	----
	60	345	---	208	----	360	---	240	----	95	----
	120	351	---	258	----	363	---	281	----	157	----
	240	300	---	262	----	327	---	272	----	200	----
	480	183	---	187	----	185	---	167	----	180	----
	960	140	---	140	----	127	---	105	----	115	----
	1920	108	---	99	----	90	---	83	----	78	----
	3480	78	8.5	74	13.0	72	8.5	64	12.0	58	17.5
1877	0	71	8.5	66	13.0	72	8.5	60	12.0	52	17.5
	10	205	---	66	----	63	---	60	----	56	----
	20	222	---	68	----	130	---	69	----	56	----
	30	307	---	82	----	250	---	85	----	56	----
	40	423	---	98	----	415	---	128	----	56	----
	50	443	---	142	----	550	---	190	----	45	----
	60	495	---	175	----	597	---	261	----	77	----
	90	410	---	250	----	600	---	350	----	113	----
	120	348	---	287	----	567	---	390	----	172	----
	240	175	---	331	----	447	---	372	----	260	----
	480	140	---	293	----	355	---	308	----	262	----
	960	227	---	208	----	258	---	237	----	216	----
	1920	235	---	157	----	177	---	163	----	155	----
	3980	108	7.0	126	13.0	115	6.0	107	11.0	101	14.5
1879	0	80	7.0	75	13.0	82	6.0	72	11.0	63	14.5
	10	253	---	152	----	251	---	84	----	67	----
	20	325	---	177	----	521	---	127	----	63	----
	30	464	---	177	----	874	---	215	----	67	----
	40	503	---	197	----	1232	---	342	----	79	----
	50	215	---	293	----	863	---	517	----	177	----
	60	263	---	304	----	820	---	532	----	191	----
	90	260	---	342	----	720	---	508	----	207	----
	120	263	---	377	----	661	---	508	----	249	----
	240	130	---	182	----	480	---	410	----	310	----
	480	256	---	192	----	352	---	304	----	280	----
	900	218	---	173	----	228	---	185	----	193	----
	1800	143	---	147	----	139	---	116	----	125	----
	3600	98	6.5	93	13.0	99	[a]4.0	86	7.0	77	15.0

[a] In char layer.

14

AND THERMOCOUPLE RADIAL DISTANCE FROM INNER SURFACE

nozzle 10.

	Plane A (1/2 in. from nozzle exit)									Nozzle exit pressure, mm Hg abs
	Thermocouple										
	8		9		10		11		12		
	Temperature, °F	Distance from inner surface, mm	Temperature, °F	Distance from inner surface, mm	Temperature, °F	Distance from inner surface, mm	Temperature, °F	Distance from inner surface, mm	Temperature, °F	Distance from inner surface, mm	
	60	23.5	65	23.0	70	7.0	63	13.0	65	19.0	---
	61	----	65	----	66	---	63	----	65	----	---
	65	----	67	----	72	---	60	----	65	----	---
	63	----	67	----	114	---	63	----	65	----	---
	61	----	67	----	186	---	70	----	65	----	2
	70	----	70	----	300	---	115	----	65	----	26
	80	----	132	----	192	---	285	----	160	----	53
	115	----	169	----	182	---	337	----	---	----	107
	188	----	203	----	154	---	318	----	254	----	151
	171	----	152	----	126	---	172	----	166	----	109
	118	----	102	----	92	---	110	----	108	----	---
	88	----	81	----	83	---	81	----	84	----	---
	70	23.5	72	23.0	71	7.0	69	12.5	61	18.5	---
	70	23.5	72	23.0	72	7.0	62	12.5	72	18.5	---
	68	----	72	----	300	---	66	----	72	----	---
	68	----	72	----	576	---	69	----	72	----	---
	67	----	70	----	750	---	82	----	72	----	---
	67	----	70	----	718	---	123	----	76	----	---
	70	----	70	----	670	---	202	----	78	----	---
	70	----	83	----	598	---	284	----	130	----	6
	88	----	132	----	118	---	405	----	203	----	29
	100	----	148	----	115	---	448	----	123	----	12
	194	----	226	----	105	---	449	----	333	----	<1
	235	----	227	----	200	---	361	----	303	----	<1
	207	----	197	----	272	---	258	----	237	----	<1
	159	----	152	----	175	---	170	----	168	----	<1
	111	23.5	106	20.5	73	[a]6.0	112	9.5	113	18.0	<1
	73	23.5	75	20.5	85	[a]6.0	84	9.5	80	18.0	756
	75	----	76	----	438	---	90	----	84	----	619
	70	----	73	----	827	---	128	----	80	----	629
	69	----	74	----	1200	---	202	----	80	----	630
	72	----	75	----	1445	---	296	----	95	----	760
	88	----	118	----	142	---	560	----	200	----	760
	93	----	127	----	135	---	568	----	220	----	12
	132	----	170	----	133	---	605	----	300	----	10
	172	----	222	----	140	---	603	----	347	----	13
	237	----	259	----	110	---	507	----	384	----	21
	260	----	231	----	105	---	332	----	302	----	23
	207	----	175	----	85	---	200	----	224	----	25
	162	----	120	----	110	---	128	----	145	----	24
	92	22.5	95	18.5	80	[a]3.0	90	9.5	98	17.5	24

15

TABLE I. - Concluded. INTERNAL-WALL TEMPERATURES

(b) Concluded.

Run	Time after start of run, sec	Plane C (2 in. from nozzle exit)				Plane B (1 in. from nozzle exit)					
		Thermocouple									
		3		4		5		6		7	
		Temperature, °F	Distance from inner surface, mm	Temperature, °F	Distance from inner surface, mm	Temperature, °F	Distance from inner surface, mm	Temperature, °F	Distance from inner surface, mm	Temperature, °F	Distance from inner surface, mm
1881	0	79	6.5	77	13.0	89	[a]4.0	87	7.0	68	15.0
	5	163	---	78	----	373	---	113	----	67	----
	10	219	---	145	----	860	---	191	----	67	----
	20	347	---	163	----	1533	---	343	----	71	----
	30	608	---	187	----	1868	---	605	----	77	----
	40	784	---	210	-----	>2200	---	826	----	99	----
	50	852	---	260	-----	1477	---	920	----	142	----
	60	582	---	272	-----	1272	---	839	----	188	----
	90	305	---	338	-----	933	---	752	----	260	----
	120	177	---	392	-----	860	---	700	----	301	----
	240	142	---	172	----	596	---	555	----	355	----
	480	159	---	134	----	427	---	431	----	325	----
	900	215	---	107	----	284	---	287	----	256	----
	1800	235	---	157	----	177	---	178	----	172	----
	3600	120	[a]6.0	117	12.5	116	[a]2.0	115	[a]6.0	99	11.5
1883	0	---	[a]6.0	74	12.5	100	[a]2.0	---	[a]6.0	25	11.5
	5	165	---	76	----	1443	---	251	----	22	----
	10	310	---	188	----	1910	---	372	----	29	----
	20	645	---	200	----	2350	---	692	----	40	----
	30	865	---	202	----	1740	---	983	----	77	----
	40	890	---	230	-----	2350	---	1164	----	103	----
	50	880	---	245	-----	2140	---	1195	----	120	----
	60	895	---	303	-----	1565	---	1114	----	155	----
	90	120	---	330	-----	1180	---	885	----	170	----
	120	100	---	300	-----	990	---	818	----	252	----
	240	90	---	153	----	650	---	601	----	300	----
	480	65	---	125	----	410	---	426	----	155	----
	900	75	---	112	----	245	---	265	----	119	----
	1800	80	---	137	----	110	---	157	----	92	----
	3000	60	[a]6.5	102	12.5	100	[a]2.0	115	[a]5.5	50	11.5
1885	0	40	[a]6.5	73	12.5	115	[a]2.0	77	[a]5.5	57	11.5
	5	190	---	71	----	---	---	200	----	56	----
	10	225	---	173	-----	---	---	254	----	67	----
	20	650	---	197	----	---	---	630	----	69	----
	30	1010	---	232	----	---	---	891	----	77	----
	40	1165	---	259	----	---	---	1045	----	80	----
	50	1095	---	320	----	---	---	1090	----	50	----
	60	550	---	385	----	---	---	923	----	88	----
	90	250	---	305	----	---	---	850	----	60	----
	120	140	---	162	----	1060	---	761	----	100	----
	240	390	---	300	----	570	---	461	----	130	----
	480	290	---	297	----	450	---	364	----	130	----
	900	40	---	101	----	335	---	275	----	100	----
	1800	40	---	85	----	225	---	137	----	71	----
	3600	40	[a]5.0	92	10.0	150	[a]3.0	101	[a]5.5	71	10.0

[a]In char layer.

16

Ablation nozzle 10.

| | | | | Plane A (1/2 in. from nozzle exit) | | | | | | Nozzle exit pressure, mm Hg abs |
| | | | | Thermocouple | | | | | | |
| 8 | | 9 | | 10 | | 11 | | 12 | | |
Temperature, °F	Distance from inner surface, mm	Temperature, °F	Distance from inner surface, mm	Temperature, °F	Distance from inner surface, mm	Temperature, °F	Distance from inner surface, mm	Temperature, °F	Distance from inner surface, mm	
76	22.5	--	18.5	92	[a]3.0	87	9.5	84	17.5	753
78	----	--	----	860	---	87	----	83	----	622
76	----	--	----	1418	---	91	----	83	----	625
94	----	--	----	1923	---	---	----	87	----	623
76	----	--	----	2147	---	307	----	84	----	624
82	----	--	----	>2400	---	458	----	101	----	752
85	----	--	----	1515	---	660	----	125	----	755
83	----	--	----	1225	---	684	----	162	----	12
108	----	--	----	950	---	705	----	260	----	13
148	----	--	----	856	---	693	----	323	----	13
253	----	--	----	658	---	585	----	402	----	22
282	----	--	----	466	---	437	----	361	----	28
226	----	--	----	139	---	293	----	253	----	31
158	----	--	----	169	---	185	----	164	----	31
111	21.5	--	16.5	113	[a]1.5	117	[a]5.5	111	16.5	8
74	21.5	--	16.5	119	[a]1.5	113	[a]5.5	85	16.5	---
70	----	--	----	2085	---	160	----	88	----	---
74	----	--	----	2230	---	239	----	92	----	---
72	----	--	----	2350	---	360	----	88	----	---
72	----	--	----	2455	---	535	----	98	----	---
76	----	--	----	2450	---	644	----	125	----	---
90	----	--	----	2190	---	680	----	125	----	---
86	----	--	----	1585	---	781	----	178	----	2
110	----	--	----	1215	---	725	----	235	----	4
154	----	--	----	1040	---	696	----	306	----	6
270	----	--	----	729	---	600	----	405	----	54
276	----	--	----	453	---	407	----	346	----	61
230	----	--	----	230	---	252	----	231	----	66
145	----	--	----	110	---	152	----	147	----	17
27	20.5	--	15.0	59	[a]1.5	107	[a]5.5	107	15.5	2
71	20.5	--	15.0	65	[a]1.5	80	[a]5.5	75	15.5	760
71	----	--	----	1650	---	132	----	76	----	625
72	----	--	----	1920	---	232	----	76	----	623
77	----	--	----	2300	---	437	----	77	----	623
83	----	--	----	2270	---	795	----	92	----	641
92	----	--	----	2250	---	1155	----	125	----	761
90	----	--	----	1630	---	1080	----	180	----	759
95	----	--	----	1300	---	942	----	230	----	26
105	----	--	----	1110	---	855	----	360	----	53
113	----	--	----	965	---	797	----	426	----	102
159	----	--	----	500	---	486	----	413	----	99
178	----	--	----	375	---	381	----	335	----	61
169	----	--	----	255	---	168	----	275	----	22
134	----	--	----	110	---	113	----	145	----	7
92	16.5	--	16.0	83	[a]1.0	100	[a]4.0	100	11.5	4

TABLE II. - EXPERIMENTAL DATA AND POSTRUN PHYSICAL DIMENSIONS FOR ABLATION NOZZLES 9 AND 10

Nozzle	Run	Run duration, sec	Accumulated run time, sec	Chamber-pressure range, lb/sq in. abs	Fuel range, percent by weight	Characteristic velocity ft/sec	percent of theoretical	Plane A (1/2 in. from nozzle exit) Average char thickness, in.	Average inside surface radius, in.	Average radius growth rate, in./sec	Plane B (1 in. from nozzle exit) Average char thickness, in.	Average inside surface radius, in.	Average radius growth rate, in./sec	Plane C (2 in. from nozzle exit) Average char thickness, in.	Average inside surface radius, in.	Average radius growth rate, in./sec	Nozzle weight, g
9	Prerun	----	----	------	---------	----	--	0	0.583	-------	0	0.574	-------	0	0.783	-------	1804.3
	1875	27.8	27.8	112-110	15.6-15.7	7430	97	.181	.587	0.00014	.193	.587	0.00047	.154	.783	0	1779.5
	1878	39.1	66.9	100-96	13.5-13.0	6920	95	.209	.668	.00207	.201	.689	.00261	.240	.801	.00072	1763.8
	1880	39.7	106.6	89-79	12.4-12.1	7080	99	.279	.708	.00101	.287	.721	.00081	.299	.812	.00028	1739.8
	1882	38.8	145.4	78-75	11.6-11.8	6980	99	.268	.752	.00113	.252	.764	.00111	.276	.818	.00015	1730.1
	1884	39.3	184.7	70-66	13.4-13.6	6900	95	.225	.886	.00341	.212	.863	.00252	.228	.906	.00224	1712.5
	1886	39.1	223.8	67-64	13.1-12.3	6830	95	.240	.929	.00110	.260	.923	.00154	.248	.969	.00161	1696.0
10	Prerun	----	----	------	---------	----	--	0	0.576	-------	0	0.591	-------	0	0.788	-------	1815.0
	1876	28.9	28.9	110-109	15.6-15.7	7510	99	.205	.587	0.00038	.220	.594	0.00010	.162	.788	0	1795.8
	1877	39.0	67.9	108-98	13.9-14.4	7340	99	.213	.654	.00172	.232	.654	.00154	.228	.807	.00049	1774.0
	1879	39.7	107.6	93-83	12.8-13.3	6800	94	.240	.705	.00128	.240	.713	.00149	.252	.833	.00065	1748.6
	1881	39.8	147.4	74-71	12.3-12.0	7150	101	.268	.792	.00218	.272	.799	.00216	.292	.862	.00073	1734.4
	1883	39.0	186.4	67-65	12.4-12.7	6770	95	.268	.818	.00067	.267	.823	.00062	.311	.867	.00013	1727.2
	1885	39.4	225.8	68-61	12.0-13.1	7070	99	.260	.867	.00124	.271	.867	.00112	.291	.898	.00079	1699.5

18

Hydrogen gas supply   Helium pressurizing gas

Fuel system vent ◄   ► Oxidant system vent
                          Oxidant-tank pressure tap

Fuel line coiled and sub-   Oxidant tank submerged in
merged in liquid-nitrogen bath   liquid-nitrogen bath

                          Oxygen load line ◄

                          Oxidant orifice flowmeter

Fuel-line pressure and temperature tap   Oxidant turbine flowmeter
Fuel orifice flowmeter   Oxidant fire valve
Fuel fire valve

Vacuum pump   Fuel purge tap   Oxidant purge tap

Fuel-injection pressure   Oxidant-injection pressure
and temperature tap   and temperature tap

Cold trap   Gaseous fluorine ◄
Concentric-tube injector   Ignition-system purge tap
Chamber pressure tap   Coolant water ◄

Water-cooled chamber   Ablation nozzle being tested

                          Vacuum-pressure transducer tap

                          Zirconium oxide
                          coated 8-in. pipe

Vacuum valve   8-in.
                          vacuum
                          gate valve

/CD-7533/

Figure 1. - Propellant flow systems and vacuum environment equipment.

Concentric-
tube
injector

Water-cooled
combustion
chamber

Ablation nozzle
test piece
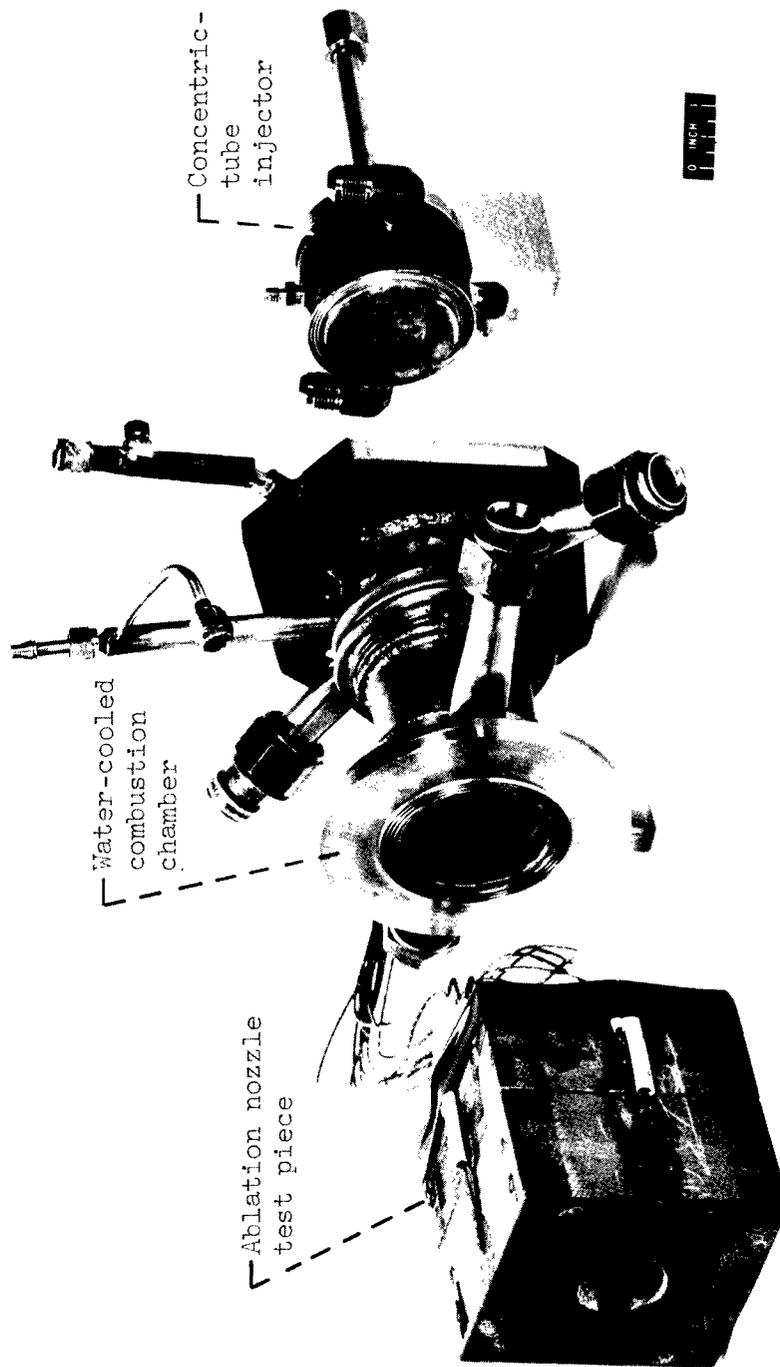
C-61422

Figure 2. - Disassembled test engine.
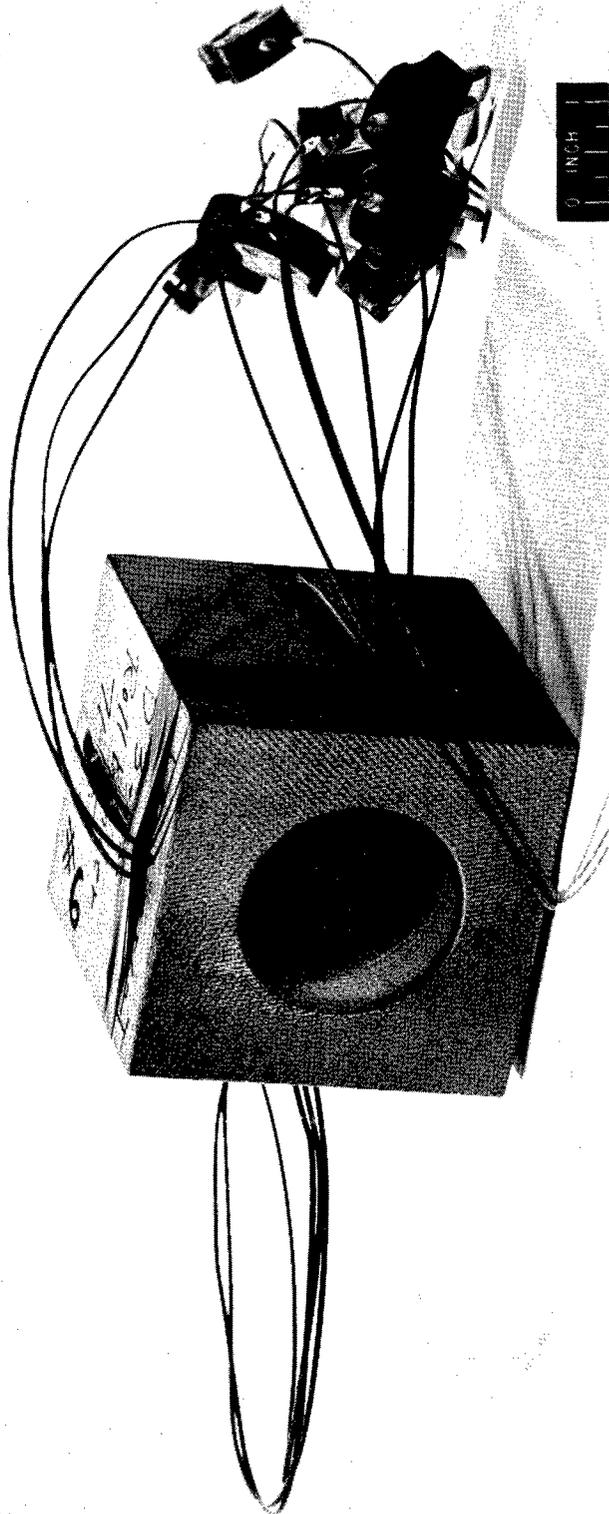
Figure 3. - Prerun ablation nozzle.

C-60529

21
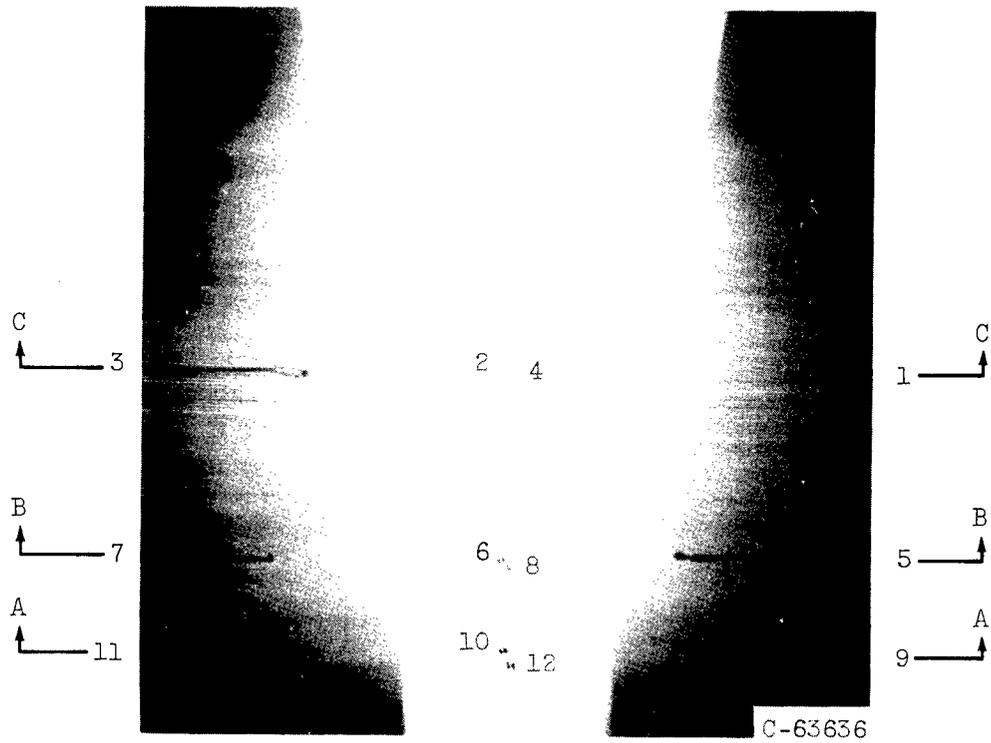
(a) Prerun nozzle.
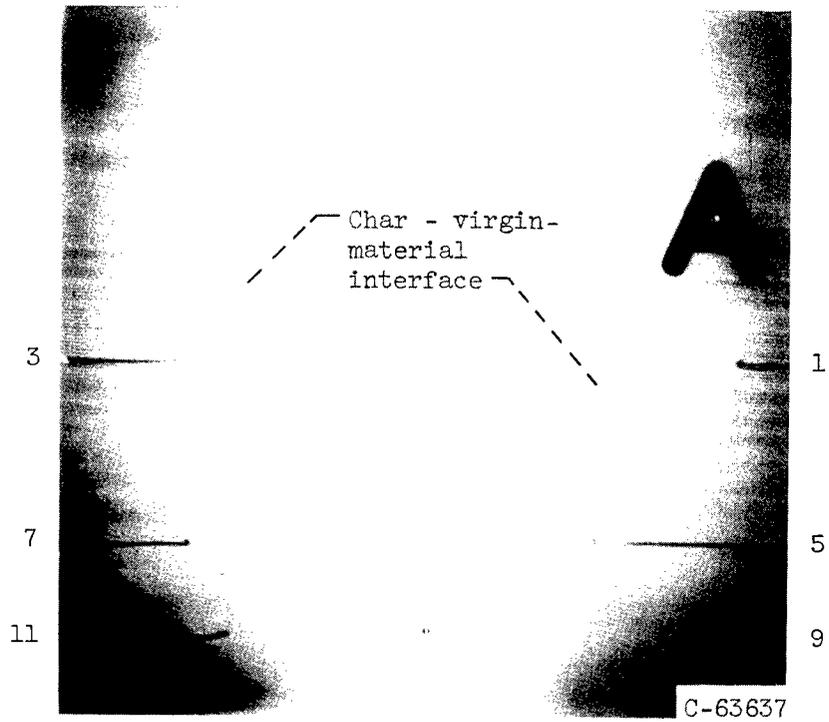
(b) Nozzle 10 after first run.

Figure 4. - X-ray of ablation nozzles. Numbers indicate thermocouples.
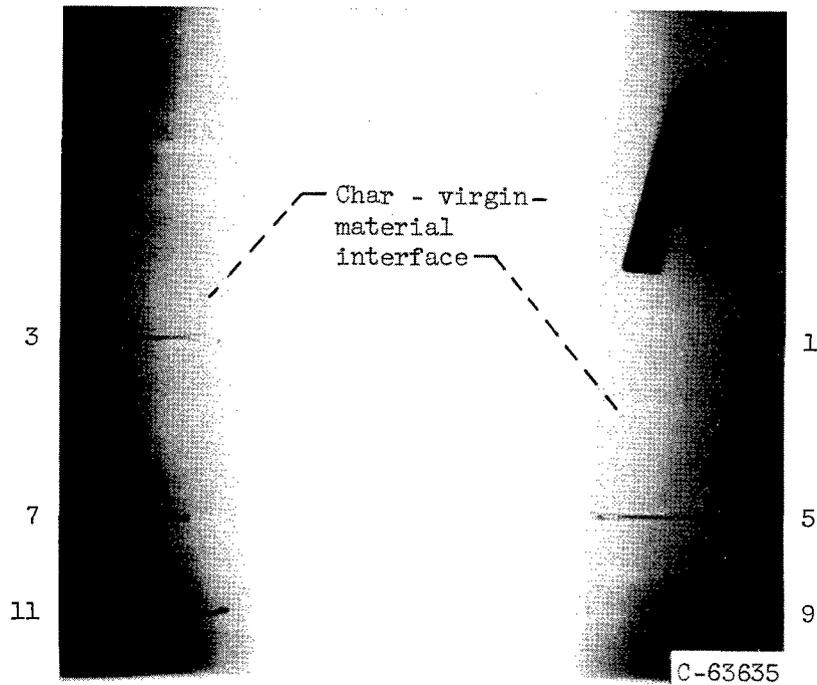
(c) Nozzle 9 after sixth and last run.
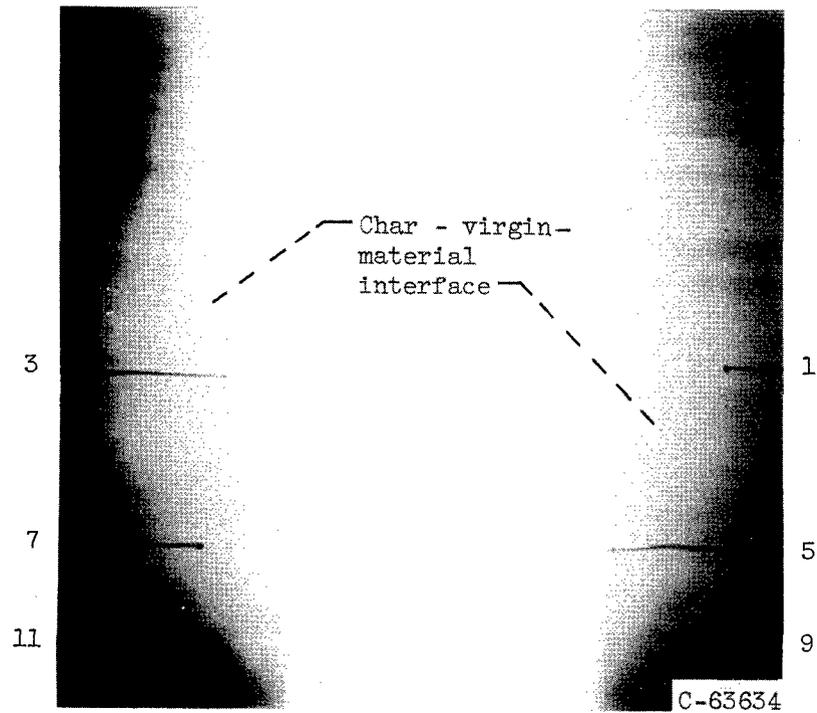
(d) Nozzle 10 after sixth and last run.

Figure 4. - Concluded. X-ray of ablation nozzles.
Numbers indicate thermocouples.

(a) Nozzle 9 oriented from combustion-chamber end.

Figure 5. - Views of nozzles 9 and 10 after sixth and last run.

C-61481
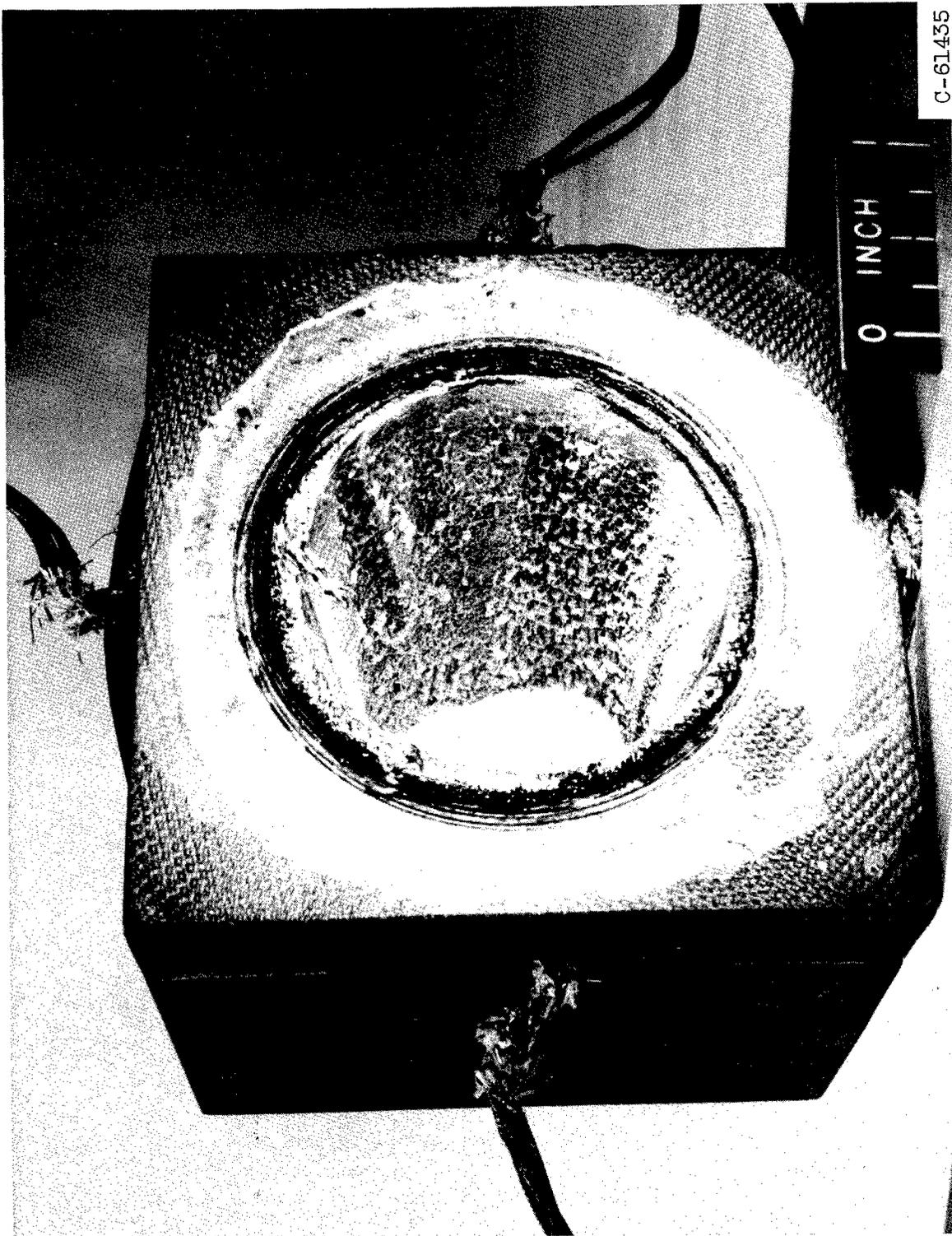
C-61435

(b) Nozzle 10 oriented from combustion-chamber end.

Figure 5. - Continued. Views of nozzles 9 and 10 after sixth and last run.
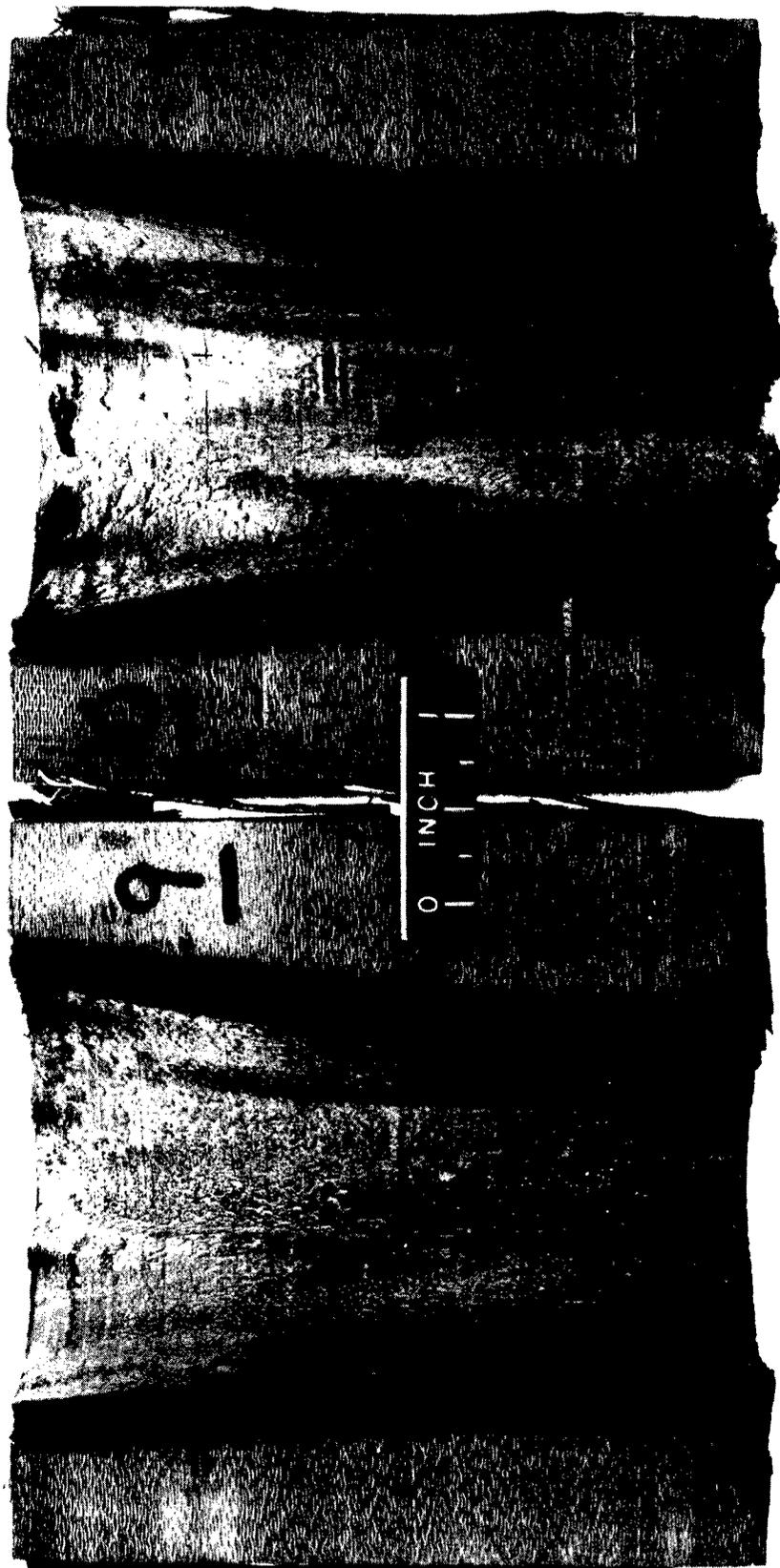
(c) Cutaway views of nozzles 9 and 10 after sixth and last runs.

Figure 5. - Concluded. Views of nozzles 9 and 10 after sixth and last run.

C-61597
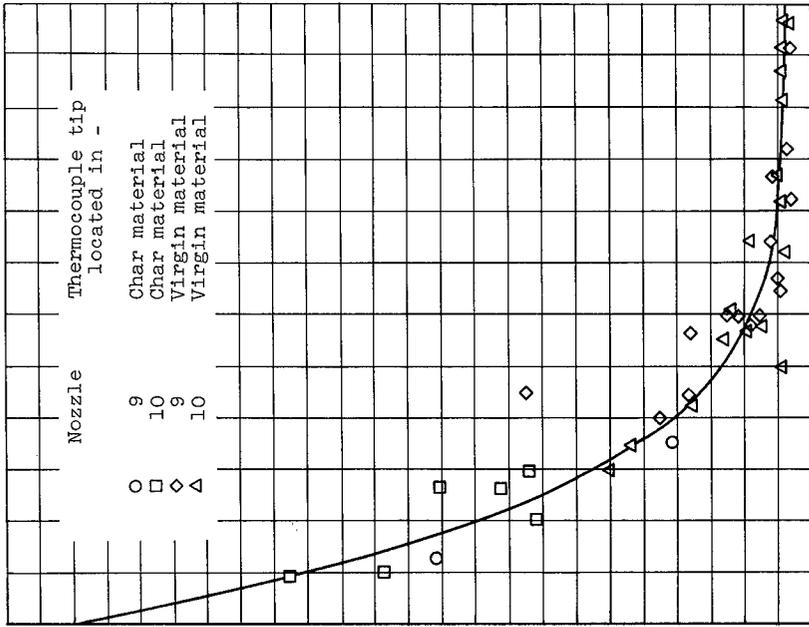
(a) 40 Seconds after start of run.
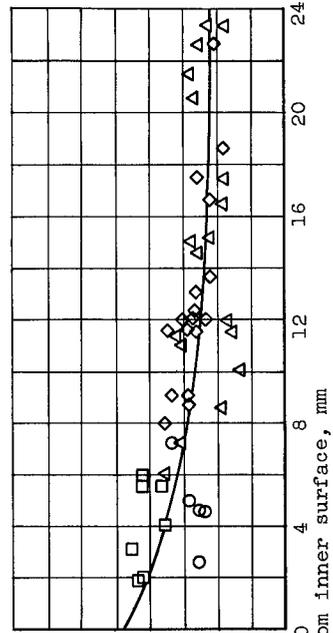
(b) 60 Seconds after start of run.
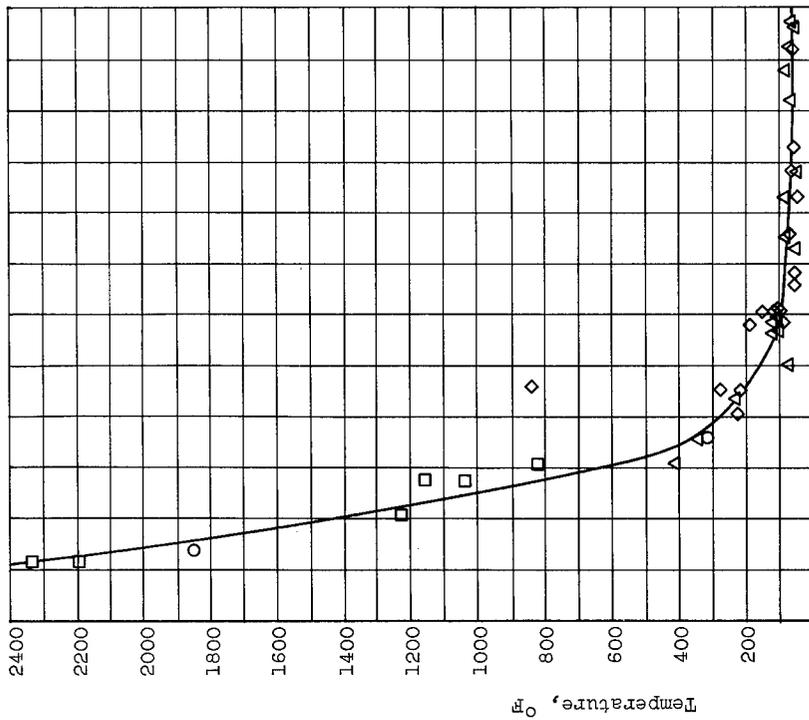
(c) 240 Seconds after start of run.
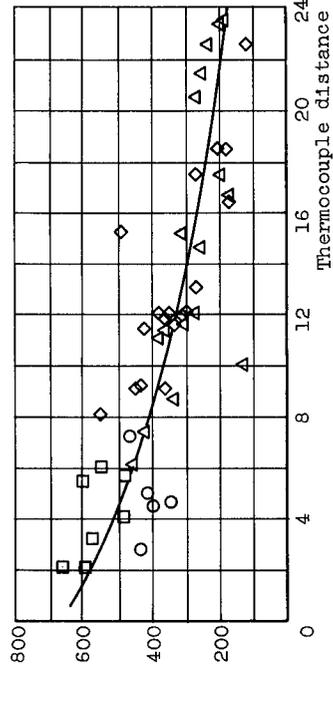
(d) 480 Seconds after start of run.

Figure 6. - Comparison of nozzle-wall temperatures as a function of distance from the hot gas surface.

27
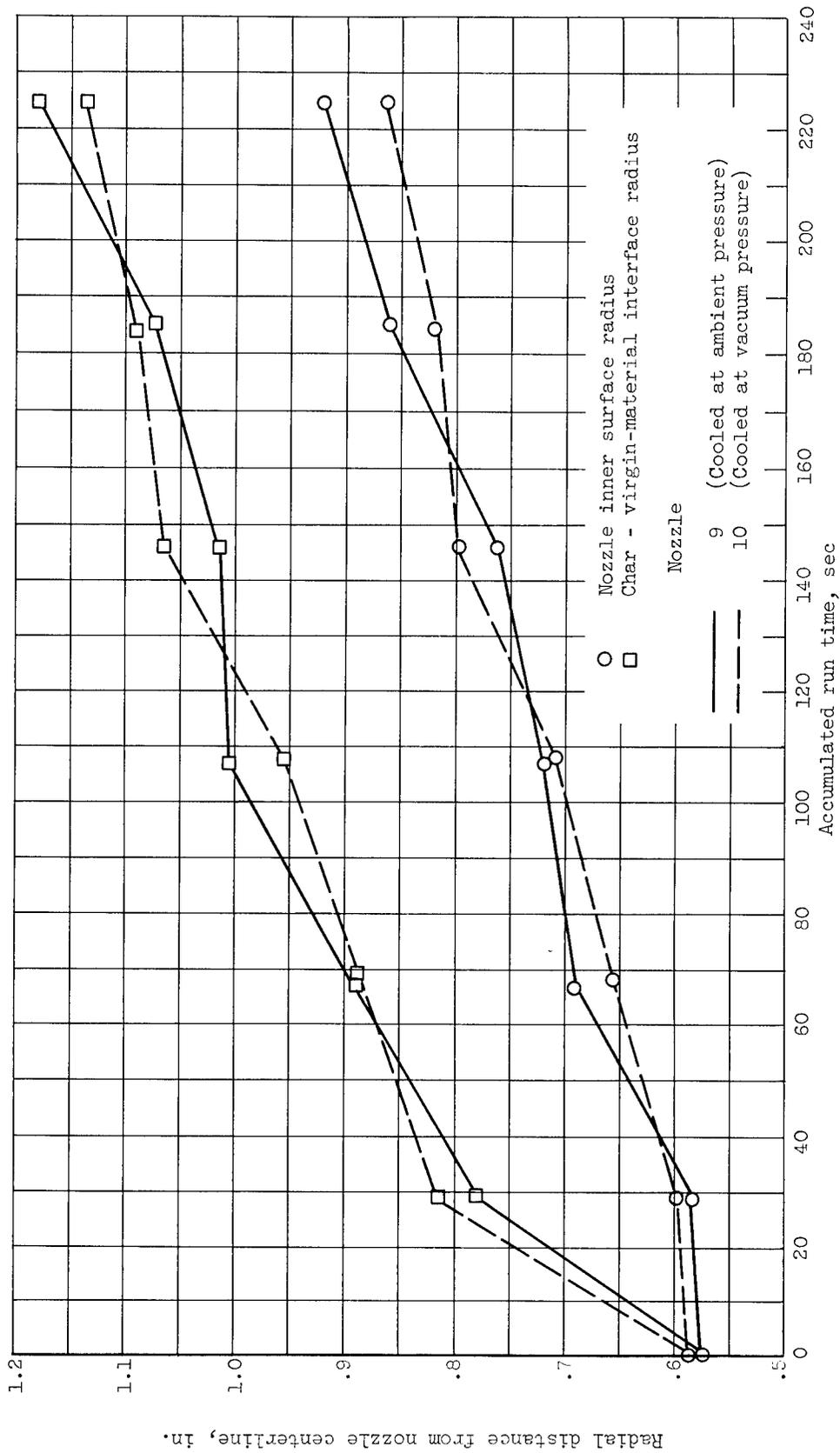
Figure 7. – Comparison of surface regression and char-layer progression for two nozzles cooled between runs at different pressures. All measurement were made at nozzle-throat entrance.
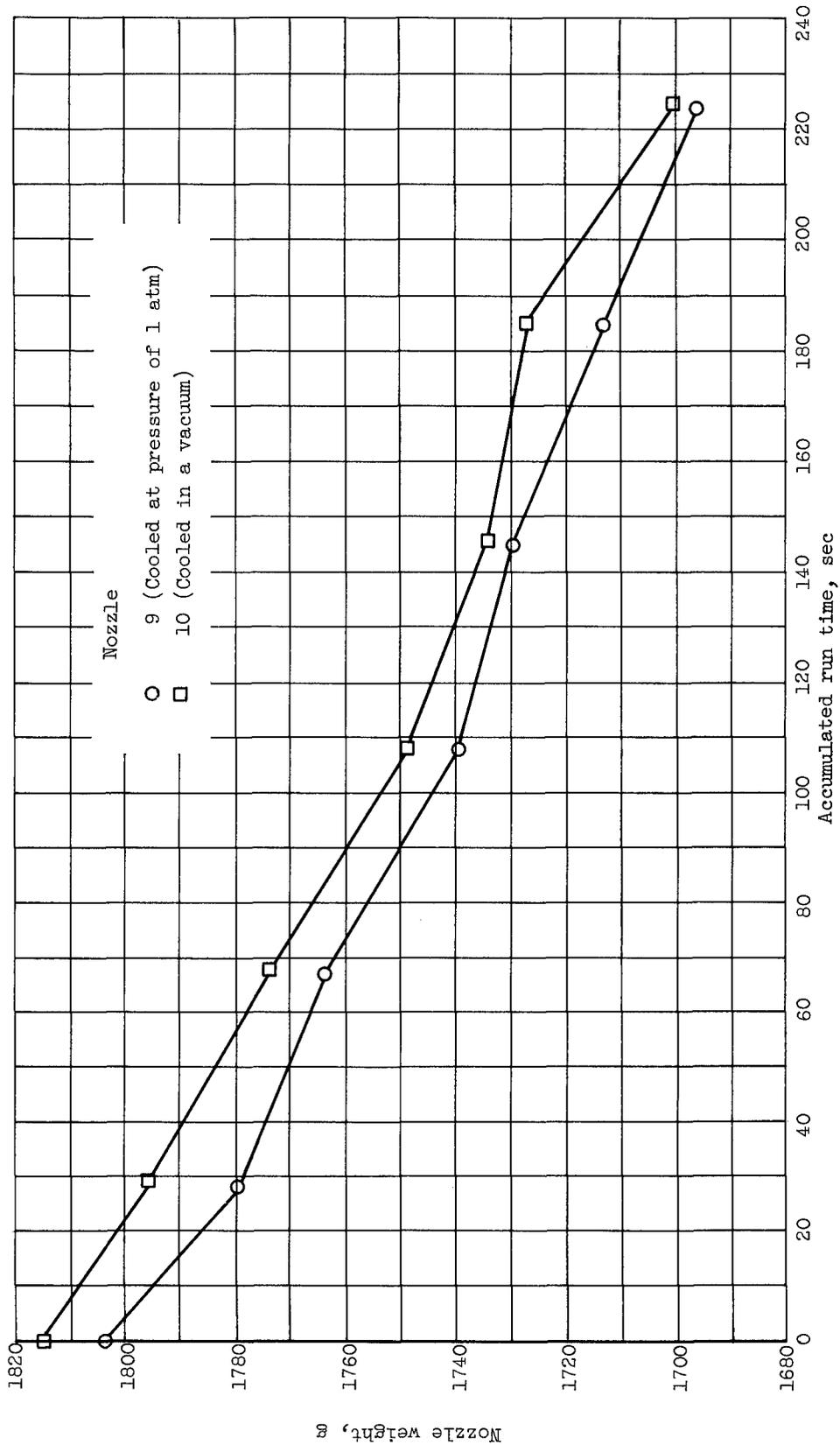
Figure 8. – Weight loss as a function of run time for two nozzles.

NASA TN D-1726
National Aeronautics and Space Administration.
EXPERIMENTAL INVESTIGATION OF ROCKET-
ENGINE ABLATIVE-MATERIAL PERFORMANCE
AFTER POSTRUN COOLING AT ALTITUDE
PRESSURES. R. James Rollbuhler. June 1963.
29p. OTS price, $0.75.
(NASA TECHNICAL NOTE D-1726)

A rocket-engine nozzle made of ablative material was
tested as part of a hydrogen-oxygen rocket engine,
which fired repeatedly in a vacuum environment.
After each run, the nozzle cooled at low pressure.
Its ablative behavior in subsequent runs did not differ
appreciably from that of an identical ablative nozzle
tested under similar conditions, but cooled at
1-atmosphere pressure.

I.   Rollbuhler, R. James
II.   NASA TN D-1726

NASA

NASA TN D-1726
National Aeronautics and Space Administration.
EXPERIMENTAL INVESTIGATION OF ROCKET-
ENGINE ABLATIVE-MATERIAL PERFORMANCE
AFTER POSTRUN COOLING AT ALTITUDE
PRESSURES. R. James Rollbuhler. June 1963.
29p. OTS price, $0.75.
(NASA TECHNICAL NOTE D-1726)

A rocket-engine nozzle made of ablative material was
tested as part of a hydrogen-oxygen rocket engine,
which fired repeatedly in a vacuum environment.
After each run, the nozzle cooled at low pressure.
Its ablative behavior in subsequent runs did not differ
appreciably from that of an identical ablative nozzle
tested under similar conditions, but cooled at
1-atmosphere pressure.

I.   Rollbuhler, R. James
II.   NASA TN D-1726

NASA

NASA TN D-1726
National Aeronautics and Space Administration.
EXPERIMENTAL INVESTIGATION OF ROCKET-
ENGINE ABLATIVE-MATERIAL PERFORMANCE
AFTER POSTRUN COOLING AT ALTITUDE
PRESSURES. R. James Rollbuhler. June 1963.
29p. OTS price, $0.75.
(NASA TECHNICAL NOTE D-1726)

A rocket-engine nozzle made of ablative material was
tested as part of a hydrogen-oxygen rocket engine,
which fired repeatedly in a vacuum environment.
After each run, the nozzle cooled at low pressure.
Its ablative behavior in subsequent runs did not differ
appreciably from that of an identical ablative nozzle
tested under similar conditions, but cooled at
1-atmosphere pressure.

I.   Rollbuhler, R. James
II.   NASA TN D-1726

NASA

NASA TN D-1726
National Aeronautics and Space Administration.
EXPERIMENTAL INVESTIGATION OF ROCKET-
ENGINE ABLATIVE-MATERIAL PERFORMANCE
AFTER POSTRUN COOLING AT ALTITUDE
PRESSURES. R. James Rollbuhler. June 1963.
29p. OTS price, $0.75.
(NASA TECHNICAL NOTE D-1726)

A rocket-engine nozzle made of ablative material was
tested as part of a hydrogen-oxygen rocket engine,
which fired repeatedly in a vacuum environment.
After each run, the nozzle cooled at low pressure.
Its ablative behavior in subsequent runs did not differ
appreciably from that of an identical ablative nozzle
tested under similar conditions, but cooled at
1-atmosphere pressure.

I.   Rollbuhler, R. James
II.   NASA TN D-1726

NASA

NASA TN D-1726
National Aeronautics and Space Administration.
EXPERIMENTAL INVESTIGATION OF ROCKET-
ENGINE ABLATIVE-MATERIAL PERFORMANCE
AFTER POSTRUN COOLING AT ALTITUDE
PRESSURES.   R. James Rollbuhler.   June 1963.
29p.   OTS price, $0.75.
(NASA TECHNICAL NOTE D-1726)

A rocket-engine nozzle made of ablative material was
tested as part of a hydrogen-oxygen rocket engine,
which fired repeatedly in a vacuum environment.
After each run, the nozzle cooled at low pressure.
Its ablative behavior in subsequent runs did not differ
appreciably from that of an identical ablative nozzle
tested under similar conditions, but cooled at
1-atmosphere pressure.

NASA

I.   Rollbuhler, R. James
II. NASA TN D-1726

NASA TN D-1726
National Aeronautics and Space Administration.
EXPERIMENTAL INVESTIGATION OF ROCKET-
ENGINE ABLATIVE-MATERIAL PERFORMANCE
AFTER POSTRUN COOLING AT ALTITUDE
PRESSURES.   R. James Rollbuhler.   June 1963.
29p.   OTS price, $0.75.
(NASA TECHNICAL NOTE D-1726)

A rocket-engine nozzle made of ablative material was
tested as part of a hydrogen-oxygen rocket engine,
which fired repeatedly in a vacuum environment.
After each run, the nozzle cooled at low pressure.
Its ablative behavior in subsequent runs did not differ
appreciably from that of an identical ablative nozzle
tested under similar conditions, but cooled at
1-atmosphere pressure.

NASA

I.   Rollbuhler, R. James
II. NASA TN D-1726

NASA TN D-1726
National Aeronautics and Space Administration.
EXPERIMENTAL INVESTIGATION OF ROCKET-
ENGINE ABLATIVE-MATERIAL PERFORMANCE
AFTER POSTRUN COOLING AT ALTITUDE
PRESSURES.   R. James Rollbuhler.   June 1963.
29p.   OTS price, $0.75.
(NASA TECHNICAL NOTE D-1726)

A rocket-engine nozzle made of ablative material was
tested as part of a hydrogen-oxygen rocket engine,
which fired repeatedly in a vacuum environment.
After each run, the nozzle cooled at low pressure.
Its ablative behavior in subsequent runs did not differ
appreciably from that of an identical ablative nozzle
tested under similar conditions, but cooled at
1-atmosphere pressure.

NASA

I.   Rollbuhler, R. James
II. NASA TN D-1726

NASA TN D-1726
National Aeronautics and Space Administration.
EXPERIMENTAL INVESTIGATION OF ROCKET-
ENGINE ABLATIVE-MATERIAL PERFORMANCE
AFTER POSTRUN COOLING AT ALTITUDE
PRESSURES.   R. James Rollbuhler.   June 1963.
29p.   OTS price, $0.75.
(NASA TECHNICAL NOTE D-1726)

A rocket-engine nozzle made of ablative material was
tested as part of a hydrogen-oxygen rocket engine,
which fired repeatedly in a vacuum environment.
After each run, the nozzle cooled at low pressure.
Its ablative behavior in subsequent runs did not differ
appreciably from that of an identical ablative nozzle
tested under similar conditions, but cooled at
1-atmosphere pressure.

NASA

I.   Rollbuhler, R. James
II. NASA TN D-1726

National Aeronautics and
Space Administration

Langley Research Center
1CC NASA Road
Hampton, VA 23681-2199

Reply to Attn of:

157A   November 7, 2005

Tracey Toomey
Attn: DTIC-BC
Defense Technical Information Center
8725 John J. Kingman Road, Suite 0944
Fort Belvoir. VA 22060-6218

Subject: Response to DTIC Form 55 Inquiry for NASA-TN-D-1726

This is to inform you that the document NASA-TN-D-1725, June 1, 1963, entitled "Rocket
Engine Ablative Material Performance After Post-Run Cooling at Simulated Altitude
Pressures," is unclassified, unlimited, and publicly available.

DTIC has permission to remove the U.S. Government Only restriction on your copy of this
document. Please see the enclosed information with current metadata for this document.

If you have any further questions, please let me know.
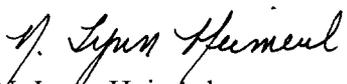
N. Lynn Heimerl   11-8-05

N. Lynn Heimerl
NASA STI Technical Publications Manager
Office of Chief Information Officer

Enclosure

November 2005

[No Title]

Author Information: Rollbuhler, R. J.

Abstract: Rocket engine ablative material performance after post-run cooling at simulated altitude pressures

Full Text: PDF

Publication Date: Jun 1, 1963

Report Number: NASA-TN-D-1726

Document ID (CASI): 19630006812

Accession Number: 63N16688

Security Classif.: Unclassified

Restriction on Access: Unlimited

Authorized Users: Publicly available

Copyright Indicator: No Copyright

Description: 29p

Imprint and Other Notes: NATIONAL AERONAUTICS ADMINISTRATION. LEWIS RESEARCH CENTER, CLEVELAND, OHIO EXPERIMENTAL INVESTIGATION OF ROCKET-ENGINE ABLATIVEMATERIAL PERFORMANCE AFTER POSTRUN COOLING AT ALTITUDE PRESSURES R. JAMES ROLLBUHLER WASHINGTON, NASA, JUNE 1963 29P 6 REFS /NASA TN D-1726/ OTS-$0.75,ABLATION; ALTITUDE; AMBIENT; CHANGE; CHAR; COOLING; EFFECT; EROSION; FIBER; INTERNAL; LAYER; LOW PRESSURE; MATCHING; NOZZLE; OXIDE; PHENOL; POSTFIRING; PRESSURE; REDUCTION; RESIN; SILICON; SIMULATION; THICKNESS; THROAT; VACUUM; WEIGHT

Available From: CASI

Format and Price Code: Hardcopy - Price Code: A03

CASI Persistent ID: hdl:2060/19630006812

Enclosure